



Science Arts & Métiers (SAM)

is an open access repository that collects the work of Arts et Métiers Institute of Technology researchers and makes it freely available over the web where possible.

This is an author-deposited version published in: <https://sam.ensam.eu>
Handle ID: <http://hdl.handle.net/10985/10779>

To cite this version :

Anthony THUAULT, Bernadette DOMENGÉS, Isabel HERVAS, Moussa GOMINA - Investigation of the internal structure of flax fibre cell walls by transmission electron microscopy - Investigation of the internal structure of flax fibre cell walls by transmission electron microscopy - Vol. 22, n°6, p.12 - 2015

Any correspondence concerning this service should be sent to the repository

Administrator : scienceouverte@ensam.eu



Investigation of the internal structure of flax fibre cell walls by transmission electron microscopy

Anthony Thuault · Bernadette Domengès ·
Isabel Hervas · Moussa Gomina

Abstract The development of the use of flax fibre as reinforcement of eco-friendly composite materials requires a good knowledge of its hydrothermal and mechanical behaviours. To this end the fibre internal structure must be finely investigated. Transmission electron microscopy was used to analyse the morphology of the fibre cell walls in terms of the arrangement of the layers and their thickness. Thus, an alternative eco-friendly staining method, based on oolong tea extract was successfully implemented. The results reveal an arrangement at the nanoscale slightly different from the classical four layer model encountered in the literature: the inner layer includes three to four sub-layers. The cell walls comprises two outer layers of relative thickness of about 10 %, a middle

layer of about 70 % and a group of thinner layers (called sub-layers) that are contiguous to the lumen with relative thickness of about 20 %.

Keywords Flax fibre · Microstructure · Transmission electron microscopy · Cell wall · Oolong tea extract staining · Cellulose

Introduction

With the growing environmental preoccupations, great efforts are devoted to the development of eco-friendly materials. Their ecological dimension involves the judicious choice of the constituents and the manufacturing process. In this context, plant fibres are very interesting for the reinforcement of polymer-matrix composites, and among them flax occupies a special position. Indeed, flax is not a food plant and the fibres present good mechanical properties: the tensile strength σ_R is in the range 400–2000 MPa, ultimate strain ε_R is between 1.2 and 3 %, the Young's modulus E between 30 and 110 GPa (Baley 2002; Batra 1998; Beukers and van Hinte 2005; Davies and Bruce 1998; Ganster and Fink 1999; Van den Oever et al. 2000; Oksman 2001; Sridhar et al. 1982; Tröger et al. 1998; Van de Velde and Kiekens 2001). The values for E-glass fibres are: $\sigma_R = 3400$ MPa, $\varepsilon_R = 4.8$ % and $E = 73$ GPa. Therefore, flax fibres possess specific mechanical properties comparable to those of glass fibres, which make this fibre an interesting material for

A. Thuault · I. Hervas · M. Gomina
CRISMAT, 6 Boulevard du Maréchal Juin, 14050 Caen,
France

A. Thuault (✉)
LMCPA, boulevard Général de Gaulle, 59600 Maubeuge,
France
e-mail: anthony.thuault@univ-valenciennes.fr

B. Domengès
LAMIPS, Joint Laboratory Presto Engineering,
CRISMAT, 2 rue de la Girafe, BP 5120,
14079 Caen Cedex, France

I. Hervas
MSMP, Arts et Métiers ParisTech, Centre de Lille, 8,
Boulevard Louis XIV, 59000 Lille Cedex, France

reinforcement in composite materials (Dittenber and GangaRao 2012; Yan et al. 2014a). Thus, due to the low density of the flax fibres compared to synthetic fibres, lighter materials can be produced ($\sim 1.4 \text{ g cm}^{-3}$ for flax fibre, $\sim 2.54 \text{ g cm}^{-3}$ for glass fibre and $\sim 2 \text{ g cm}^{-3}$ for carbon fibres (Baley 2002; Batra 1998; Davies and Bruce 1998; Ganster and Fink 1999; Tröger et al. 1998). Mass saving is sought in many fields of applications such as automotive, nautical and aeronautic since it means energy saving. In addition to their high specific mechanical properties, their natural character, their annual turnover and low environmental impact production of these fibers are very interesting materials. Currently, flax fibres/epoxy composites are strongly investigated for automotive engineering applications. Indeed, they present interesting mechanical properties comparable to those obtain for glass fibres/epoxy composites: compressive strength 77.5–299.6 MPa, tensile strength 63–92.6 MPa, interlaminar shear strength 10.7–23.3 MPa and specific energy absorption 21.2–34.2 kJ/kg (Meredith et al. 2012, 2013; Yan and Chouw 2013; Yan et al. 2014b, 2014c). In the construction field, research is underway to the association of plant fibers to cementitious materials, like cementitious composites with glass fibers. However, the biochemical composition of these fibers delays the setting, their hydrophilic character affects the hydration of the cement and the workability of the mixture is unsuitable for many applications (Juarez et al. 2007; Olorunnisola 2008; Pacheco-Torgal and Jalali 2011; Sawsen et al. 2014, 2015). However, the mechanical properties of the fibres present a significant variability when they are exposed to UV or water and decrease between 10 and 30 % (Le Duigou et al. 2015; Thuault et al. 2013a; Yan et al. 2015). Thus, flax fibre has the potential to be used as reinforcement for construction and building composite materials if this variability is taken into account.

In the stem, flax fibres are organized in bundles located between the phloem and the xylem of the stem. The ultimate fibre has an average length of 10–40 mm and an average diameter between 10 and 30 μm (Batra 1998; Mukherjee and Satyanarayana 1986a; Wang et al. 2001). Its microscopic structure can be sketched out as a tubular cylinder with a central cavity, the lumen (Fig. 1). On the nanoscale the flax fibre is made of two cell walls: the primary one is very thin and the secondary is classically subdivided into three layers from outer to inner: S1, S2 (the thickest) and S3

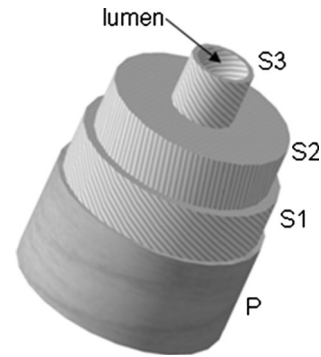


Fig. 1 Usual representation of the flax fibre cell wall arrangement

[(Baley et al. 2005; Bos and Donald 1999; Brett and Waldron 1996; Nilsson and Gustafsson 2007; Preston 1974; Roland et al. 1995).

Hence, flax fibre can be considered as a composite structure for which the reinforcement is the crystalline cellulose microfibrils (Fink et al. 1999; Gassan et al. 2001; Lennholm et al. 1994; Saxena and Brown 2005; Weimer et al. 1990), embedded in an amorphous matrix mainly made of hemicelluloses and pectins and structural water (Fig. 2). Fibres biochemical composition was determined by using the Van Soest's method (Godin et al. 2011). The mostly crystalline cellulose is approximately 78 % of the fiber mass, hemicelluloses about 6 %, lignin about 5 %, pectins about 3 % and water about 8 % (Thuault et al. 2013b). Due to their close chemical compositions, hemicelluloses constitute the interface between cellulose and pectins whereas lignin is located between the hemicellulosic areas. Water is mainly linked to the hemicelluloses due their numerous ramifications (Charlet et al. 2009).

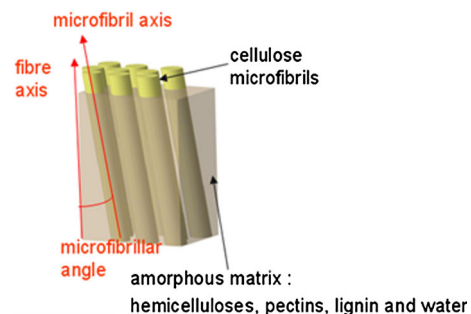


Fig. 2 Schematic representation of the arrangement of the fibre components

It should be noted that all morphological, biochemical and mechanical properties of the flax fibre exhibit a large dispersion; they are known to depend on the considered variety, the soil quality, the climatic conditions during the growth, the maturation degree of the plant, and the decortication conditions (Charlet et al. 2007, 2009). Finally, the cellulose microfibrils are organized in layers in a helical fashion along the axis of the fibre. The microfibrils angle with the longitudinal axis of the fibre, which strongly influences the mechanical properties, is estimated to about 10° in the thickest layer S2 and between 30° and 60° in S1 and S3 (the lower the angle, the better the mechanical properties are) whereas microfibrils are randomly disposed within the external P wall (Chakravarty and Hearle 1967; Hearle 1963; Mukherjee and Satyanarayana 1986a, b; Roe and Ansell 1985; Stout and Jenkins 1955; Wang et al. 2001).

To the authors' knowledge, all previous TEM studies of flax fibres (which are non-lignified fibres) aimed exclusively at investigating the polysaccharides organization. However, TEM is a powerful tool with the resolution required for detailed observation and measurement of all the layers in the cell walls, as it had been highlighted on wood fibres (Fromm et al. 2003; Lehringer et al. 2009). Therefore, the fibres were submitted to PATAg (periodic acid thiocarbonylhydrazide silver proteinate) test, which allows polysaccharides detection, or the usual uranyl acetate/lead citrate method. Moreover, cell walls organization in flax fibre has not been specifically investigated yet: the data reported in the literature were extrapolated from the study of lignified fibre cell walls such as wood.

In this study, the internal structure of the flax fibre is investigated using transmission electron microscopy (TEM) and a special attention is paid to the number of layers and their respective thickness. These parameters are required for modelling the morphology of the fibre in order to simulate its mechanical and hygrothermal behaviour. Using focused ion beam (FIB) Microscopy observations, Domenges and Charlet (2010) proposed a description of the layers arrangement in the cell walls slightly different from that of the conventional four layer model (Mark 1967) P/S1/S2/S3. Indeed, they have observed an external wall (very thin, less than $1\ \mu\text{m}$), a thick intermediate layer and a less thick internal layer made of four sub-layers.

In this work the original staining method based on oolong tea extract (OTE) and used herein to prepare

the thin cross sections is detailed. Then the results of the TEM analyses are presented, the cell walls organisation is discussed and compared to the findings revealed by FIB microscopy.

Experimental

Material—flax fibre

Flax fibres from the Institut Technique du Lin (France) were Agatha variety of *Linum usitatissimum*, one of the most cultivated varieties in Europe. They originate from plants grown in the same field, the same year in the same cultural conditions. In the field, the plants ripped from the ground are exposed to sun and rain (dew-retting) and that promotes the ingestion of pectins which separate the fibre bundles from the xylem (Barbulée et al. 2014). Then, the stems were scutched to be stored under conditions of controlled temperature and humidity (21°C , 64 % RH). Finally, ultimate fibres were manually extracted from bundles located in the middle of the stem, as it had been shown that their properties are higher than those of fibres extracted from the top or the bottom of the stem (Charlet et al. 2007, 2009), to undergo metallographic preparation for TEM analyses. The average fibre diameter was evaluated by the mean of six measurements taken along the fibre using an optical microscope. 120 fibres were considered and an average diameter of $20.8 \pm 5.9\ \mu\text{m}$ was obtained. The fibre density was determined by using an helium pycnometer: $1.43 \pm 0.01\ \text{g cm}^{-3}$. The mechanical properties (strength, ultimate strain and Young's modulus) of the fibres were obtained from tensile tests with a gauge length of 10 mm, using a universal testing machine equipped with a 2 N capacity load cell. The tests were run at a crosshead displacement rate of 1 mm/min, as it was described in previous papers (Charlet et al. 2007, 2009). At room hygrothermal conditions (52 % relative humidity, 23°C) the following values were obtained: tensile strength $\sigma = 875.9 \pm 147.4\ \text{MPa}$, Young's modulus $E = 59 \pm 9.7\ \text{GPa}$ and ultimate strain $\epsilon = 2.5 \pm 0.8\ \%$.

Cross section preparation

TEM lamellae were prepared using classical embedding and ultra-microtomy. The fibres were embedded

in a resin in order to ease the cross-sectioning. Then, transversal cross sections were cut using an ultramicrotome (Leica EMUG7 model) equipped with a glass knife (cryotim 45 type) for coarse cuts, and a diamond knife (ultra Atomic Force Microscopy type) for fine cuts. Cross sections of about 70 nm in thickness were obtained and picked up on a TEM 200 mesh copper grid. For this study, the cross sections of 21 ultimate flax fibres were considered.

Cross section staining

To enhance the contrast of cellular component on TEM images, ultrathin sections are usually soaked in a single drop of uranyl acetate solution and post-fixed in a solution of NaOH and lead citrate. However, uranyl acetate is a radioactive material for which supplying and use are strictly regulated. Moreover, uranyl acetate is as toxic if inhaled or ingested as lead. Furthermore, since these products are pollutants, they have a negative impact on the environment, which is contrary to the eco-friendly approach linked to the development of eco-composites materials. In this context, it seemed interesting to consider a recent staining method using OTE.

OTE is a plant-derived extract and a highly safe product constituted of polyphenols, which can be found in candies for example (Sato et al. 2008). The phenolic groups participate in the formation of hydrogen bonds with the aldehyde groups contained in hemicelluloses, in particular. Because of its high atomic mass compared to flax fibre constituents, the OTE will enhance contrast of hemicelluloses rich areas (negative staining). This method has already been successfully used to stain liver cells and the results are very similar to those obtained with the conventional uranyl acetate and lead citrate staining (Carpentier et al. 2012; Sasaki et al. 2001; Sato et al. 1996, 2003, 2008; Yamaguchi et al. 2010).

Herein, in a first step single, drops of a solution made of 0.2 % mass OTE in distilled filtered (0.22 µm filter) water were put on a paraffin film and the ultrathin sections were soaked in for 30 min at room temperature and then rinsed in distilled filtered water. The post-fixation was performed in a CO₂-free chamber to avoid any chemical reaction with the lead citrate. To this end the paraffin film in a petri dish was surrounded by NaOH pellets. The sections were dived

in single drops of a solution of 1 N NaOH and 0.1 % mass lead citrate in distilled filtered water for 4 min and then rinsed in distilled filtered water (method A). In method B, no post-fixation is carried out. The two methods are evaluated in this study.

TEM

In order to enhance contrast and minimize the irradiation damage, biological samples are usually observed at rather low voltage (Näslund et al. 1988). Here, the TEM microscope (TEM-STEM-FEG JEM 2011) was operating at 120 kV, using a cooling sample holder (liquid nitrogen temperature) in a first step. It appeared not necessary as long as observations would be performed on sample lamellae deposited close enough to a bar of the supporting 200 mesh copper grid. Those would ensure charge flooding and limit the overheating of the sample.

Results and discussion

First, it is important to note that no significant difference was observed between the cross sections stained with OTE only (method B) and those stained with OTE and post-stained with Lead Citrate (method A); in the following the staining method is indicated on each TEM image (either OTE or OTE-LC). Thus, lead citrate post-staining will not be necessary for future TEM observations. Regarding the good contrast obtained on these pictures, it can be stated that OTE staining permits to avoid the use of noxious products (lead citrate and uranyl acetate). It should be considered as a good marker of hemicelluloses rich areas, which are related to the presence of cellulose (Morvan et al. 2003).

Pictures obtained by TEM allow distinguishing the several layers constitutive of the cell walls of flax fibre. On first observations at low magnification (Fig. 3a), dark contrast residues of lead citrate are still present but it is possible to clearly identify the lumen (L), the middle lamella (ML) and several cells junctions (Cj). The investigated fibres are located in a bundle and have a diameter of about 20 µm, which is comparable to the measurements carried out by optical microscopy on ultimate fibres extracted from the bundle (Thuault et al. 2011). They exhibit polygonal shape (hexagonal) rather than circular, like it is

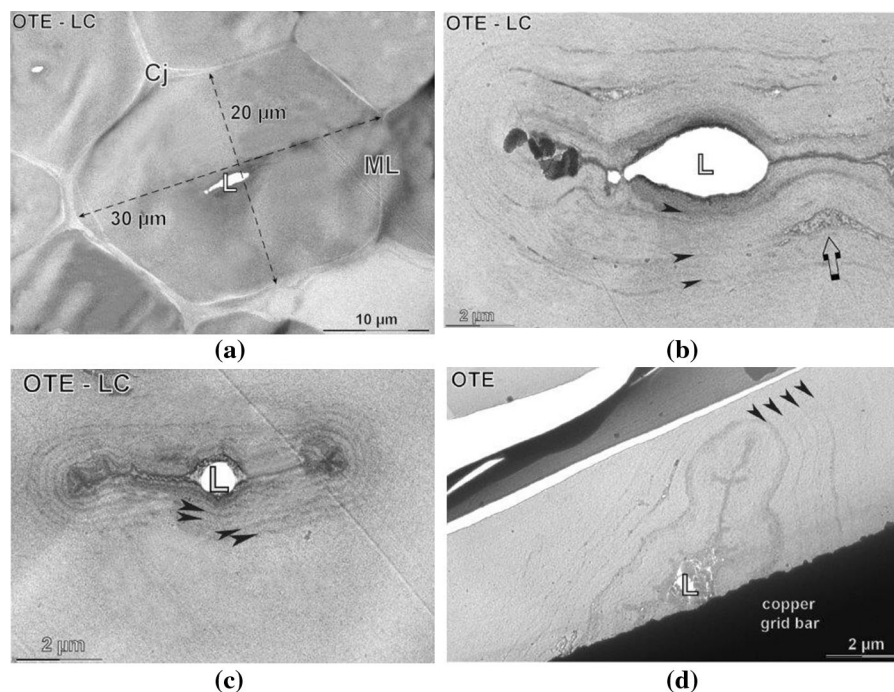


Fig. 3 TEM images of a flax fibre cross sections **a** low magnification—L (lumen), ML (middle lamella) and Cj (cell junction); **b–d** medium magnification showing three or four concentric layers around the lumen; OTE stays for OTE only

staining and OTE-LC for OTE staining plus with lead citrate post-staining (note citrate *dark gray* residues). To help visualization of the different layers, citrate residues were lightened on **b, c**

conventionally described. This is due to the strain applied by the neighbouring fibres of the bundles. Pictures at higher magnification enable to observe a remarkable feature on almost all fibres: the lumen is surrounded by a complex arrangement of three to four concentric sub-layers (Fig. 3b–d). These observations are similar to those of a former TEM study using classical staining (Morvan et al. 2003) and those made by using FIB microscopy (Domenges and Charlet 2010). FIB microscopy observations were based on imaging the irradiation damage produced by focused Ga^+ ion beam, enhancing more sensitive areas. FIB image in Fig. 4 reveals four concentric sub-layers around the lumen. Currents results confirm that this complex morphology of the sub-layers around the lumen is not related to any observation artefact, but corresponds to the true nature of the flax fibre. Besides these concentric sub-layers around the lumen, a thick intermediate layer and a very thin external one are also observed.

As the fibre diameter shows a large dispersion, it was chosen to describe the organisation and the

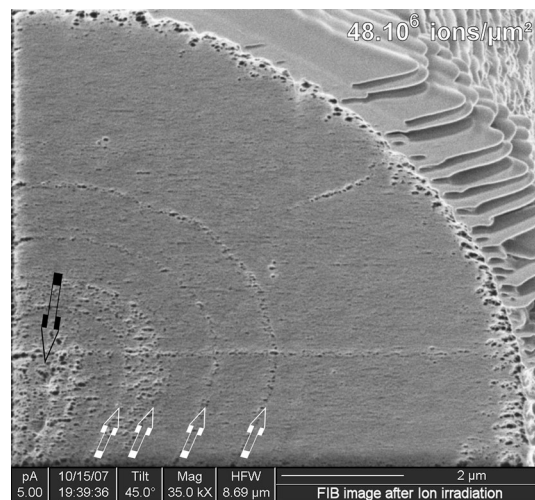


Fig. 4 FIB image of a flax fibre cross-section, after Ga^+ ion irradiation, showing the lumen (*dark arrow*) and concentric layers around the lumen (*white arrows*)

thickness of the layers relatively to the diameter (%). Some authors hypothesized the same structure for flax fibre as for wood (Baley et al. 2005; Bos and Donald

1999) and reported a relative thickness of 8–15 % for S1 and S3, 70–80 % for S2 and 1–4 % for P. Others have experimentally observed the structure of the bevelled-cut section of flax fibre (Roland et al. 1995) and highlighted three distinct layers together with the middle lamellas. However, the transition zones between S1 and S2 or S2 and S3 do not clearly appear and thus no sub-layers could be identified. Consequently, no evaluation of the layers thickness was proposed.

In this study, it has been noted that the whole concentric internal sub-layers nearest to the lumen represent about 20–25 % of the cell walls thickness while the intermediate layer represents about 55–70 % and the outer layer about 2–10 % (Fig. 5a, b). This external layer was investigated at higher magnification (Fig. 5c, d). In fact, two distinct external layers can be isolated. The inner layer, marked with white dashed lines in Fig. 5, is darker and thus probably hemicelluloses rich. Thus, the inner domain might correspond to the generally called S1 layer which is made of

70–80 % of oriented cellulose microfibrils whereas the outer domain (dark dashed lines) might be the primary cell wall P which contains less cellulose [\sim 8–14 % (Baley 2002)] and no oriented microfibrils



Fig. 6 High magnification TEM micrograph of the middle lamella of a flax fibre; S1 and primary cell wall are marked through two sets of *dashed lines*

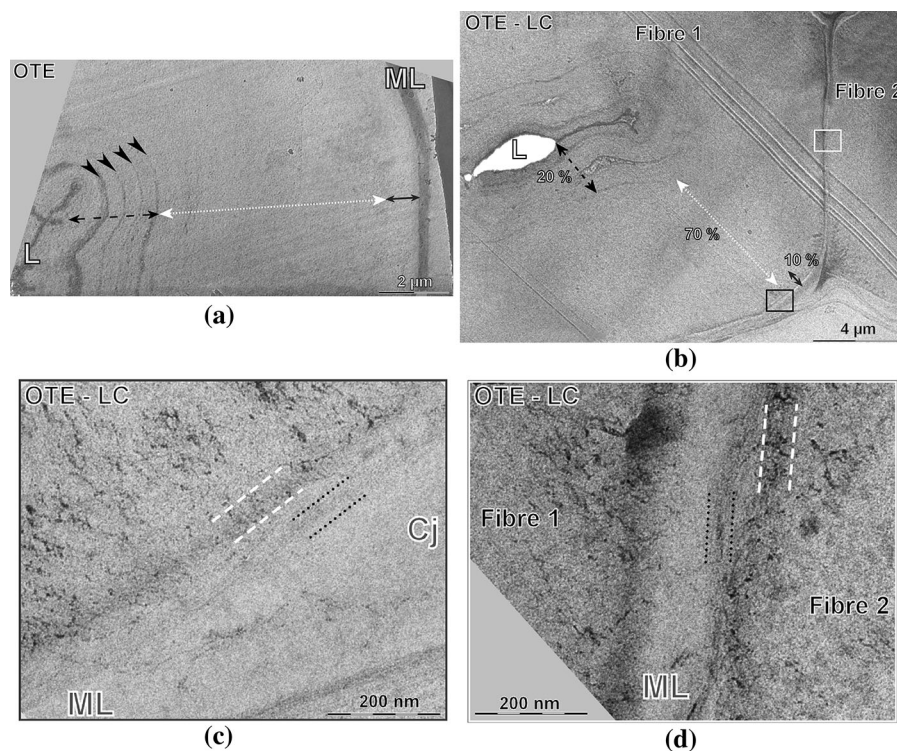


Fig. 5 a, b Medium magnification TEM micrographs showing the internal organisation of the cell-walls layers and their average relative thicknesses (*dashed double arrows*), c, d higher

magnification TEM micrographs showing the organisation of the external layer on two sites of b, darker contrast areas along the middle lamella are marked with two sets of *dashed lines*

(Chakravarty and Hearle 1967; Mukherjee and Satyanarayana 1986a, b; Stout and Jenkins 1955; Wang et al. 2001). Indeed, it exhibits a contrast similar to that of the middle lamella (Fig. 6), which suggests that they have close biochemical compositions.

These observations also permit to evaluate the thickness of the middle lamella which, to the knowledge of the authors, is not often available in the literature due to its irregular shape and to the resolution required to observe it. Thus, the middle lamella thickness ranges between 150 and 600 nm depending on the location between two adjacent fibres.

Finally, TEM also highlighted some defects in the layer organisation of the cell wall. For instance, a local disorganized area is shown on the Fig. 3b (arrowed zone). This kind of defect may have appeared due to:

- Unfavourable climatic conditions during fibre growth could have disturbed the enzymatic production and the organisation of the cellulose microfibrils by the rosettes and created a very localized zone with another biochemical arrangement (Chernova and Gorshkova 2007; Doblin et al. 2002; Gorshkova et al. 2003) (brighter areas are less dense);
- The mechanical treatments applied to the fibres when extracting them from the stem, which could have locally damaged the cell walls.
- Finally, more significant differences are noted in the inner layers for which three hypotheses can be considered:
- The so-called S3 layer should be made of three or four sub-layers evidenced above. However, the thickness of these sub-layers is higher than the S3 layer generally described in the classical four layer model;
- The S3 layer defined in the four layer model should be the inner sub-layer and the others sub-layers would be a “transition domain”. Indeed, Roland et al. (1995) have hypothesized that the change in the microfibrils angle between the layers of the cell walls should occurs gradually through transition layers. Thus, it can be suggested that the transition between S2 and S3 occurs more progressively than the transition between S1 and S2 and that may explain why transition layers cannot be observed in the latter case.
- The ultimate hypothesis would be that the usual four layer model (P/S1/S2/S3) is not accurate enough and, because of the difficulty to observe

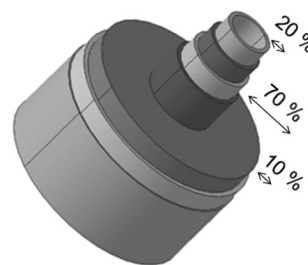


Fig. 7 Proposition for the cell wall organisation based on our TEM observations (the relative thickness is also noted)

the internal structure of the flax fibre, the complexity of the organisation of the most internal layers have not been revealed so far. In this case, it would be possible to describe a seven layers based model of the flax fibre, as shown in Fig. 7.

Finally, the progress that represents the finest determination of the morphology of the fibers is a step towards determining their fine nanostructure in terms of the location of the hydrophilic and hydrophobic phases. This permits to verify the current hypothesis and to provide data for modelling (Gorshkova et al. 1996, 2000; Morvan et al. 2003). Thus, future modelling could permit to determine the water absorption into the fibre and so to establish its consequences on the mechanical properties, since it has been evidenced that the relative humidity strongly influence the ultimate strength and the Young's modulus (Thuault et al. 2013a). Moreover, the different cell walls organisation highlighted in this study could also be used to carry out more accurate numerical simulation of the fibre mechanical behaviour (Thuault et al. 2013c). Indeed, the interface between the layers and the microfibrils angle considered for each layer would influence the fibre mechanical behaviour.

Conclusions

The flax fibre structure was investigated by TEM in order to identify its sub-morphology and quantitatively evaluate the thickness of the layers in the cell walls. OTE staining method was successfully used as an alternative to the usual staining method which makes use of noxious products. It was shown that a lead citrate post-staining treatment does not significantly improve the image contrast.

This study of the flax fibre structure allowed measuring the relative thickness of the different cell walls layers (P, S1, S2, S3). Thus, from inner to outer: S3 represents 20–25 % of the secondary cell wall thickness whereas S2 and S1 represents 55–70 % and 2–10 % respectively. Moreover, the fine analysis of the fibre outer zones allows distinguishing between the primary cell wall and the middle lamella.

Two new important results were obtained: it was possible to clearly distinguish between the primary cell wall and the middle lamella, the thickness of the latter ranges from 150 to 600 nm; this study highlighted the presence of 3 or 4 sub-layers within S3 which reflects the complex morphology of this plant fibre.

These observations and microstructural data will help to implement a numerical model of the flax fibre considered as a multilayer composite material. The association of specific mechanical properties to the different layers and sub-layers revealed in this work can be used to implement a numerical simulation of the fibre mechanical behaviour.

Acknowledgments They are grateful to the French National Research Center (CNRS) and the Region of Lower Normandy for their financial support. Authors also want to thank Dr. B. Duchemin for his helpful advices.

References

- Baley C (2002) Analysis of the flax fibres tensile behaviour and analysis of the tensile stiffness increase. *Compos A Appl Sci Manuf* 33:939–948
- Baley C, Morvan C, Grohens Y (2005) Influence of the absorbed water on the tensile strength of flax fibers. *Macromol Symp* 222:195–202
- Barbulée A, Jernot J-P, Bréard J, Gomina M (2014) Damage to flax fibre slivers under monotonic uniaxial tensile loading. *Compos A Appl Sci Manuf* 64:107–114
- Batra SK (1998). Handbook of fiber chemistry—other long vegetable fibers. In: Lewin M, Pearce EM
- Beukers A, van Hinte E (2005) Lightness: the inevitable renaissance of minimum energy structures (010 Publishers)
- Bos HL, Donald AM (1999) In situ ESEM study of the deformation of elementary flax fibres. *J Mater Sci* 34:3029–3034
- Brett CT, Waldron KW (1996) Physiology and biochemistry of plant cell walls. Chapman and Hall, Londres
- Carpentier A, Abreu S, Trichet M, Satiat-Jeunemaitre B (2012) Microwaves and tea: new tools to process plant tissue for transmission electron microscopy. *J Microsc* 247:94–105
- Chakravarty A, Hearle JWS (1967) Observations of the tensile properties of ultimate cells of some plant fibres. *J Text Inst* 58:651–656
- Charlet K, Baley C, Morvan C, Jernot JP, Gomina M, Bréard J (2007) Characteristics of Hermès flax fibres as a function of their location in the stem and properties of the derived unidirectional composites. *Compos A Appl Sci Manuf* 38:1912–1921
- Charlet K, Jernot JP, Gomina M, Bréard J, Morvan C, Baley C (2009) Influence of an Agatha flax fibre location in a stem on its mechanical, chemical and morphological properties. *Compos Sci Technol* 69:1399–1403
- Chernova T, Gorshkova T (2007) Biogenesis of plant fibers. *Russ J Dev Biol* 38:221–232
- Davies GC, Bruce DM (1998) Effect of environmental relative humidity and damage on the tensile properties of flax and nettle fibers. *Text Res J* 68:623–629
- Dittenber DB, GangaRao HV (2012) Critical review of recent publications on use of natural composites in infrastructure. *Compos A Appl Sci Manuf* 43:1419–1429
- Doblin MS, Kurek I, Jacob-Wilk D, Delmer DP (2002) Cellulose biosynthesis in plants: from genes to rosettes. *Plant Cell Physiol* 43:1407
- Domenges B, Charlet K (2010) Direct insights on flax fiber structure by focused ion beam microscopy. *Microsc Microanal* 16:175–182
- Le Duigou A, Bourmaud A, Baley C (2015) In-situ evaluation of flax fibre degradation during water ageing. *Ind Crops Prod* 70:204–210
- Fink HP, Walenta E, Kunze J (1999) The structure of natural cellulosic fibres-Part 2. The supermolecular structure of bast fibres and their changes by mercerization as revealed by X-ray diffraction and C-13-NMR-spectroscopy. *Papier* 9:534–542
- Fromm J, Rockel B, Lautner S, Windeisen E, Wanner G (2003) Lignin distribution in wood cell walls determined by TEM and backscattered SEM techniques. *J Struct Biol* 143:77–84
- Ganster J, Fink HP (1999) Physical constants of cellulose. *Polymer Handbook Immergut EH, Grulke*
- Gassan J, Chate A, Bledzki AK (2001) Calculation of elastic properties of natural fibers. *J Mater Sci* 36:3715–3720
- Godin B, Agneessens R, Gofflot S, Lamaudière S, Sinnaeve G, Gerin PA, Delcarte J (2011) Revue bibliographique sur les méthodes d'analyse des polysaccharides structuraux des biomasses lignocellulosiques. *Biotechnol Agron Soc Environ* 15:165–182
- Gorshkova TA, Wyatt SE, Salnikov VV, Gibeaut DM, Ibragimov MR, Lozovaya VV, Carpita NC (1996) Cell-wall polysaccharides of developing flax plants. *Plant Physiol* 110:721–729
- Gorshkova TA, Salnikov VV, Pogodina NM, Chemikosova SB, Yablokova EV, Ulanov AV, Ageeva MV, Van Dam JEG, Lozovaya VV (2000) Composition and distribution of cell wall phenolic compounds in flax (*Linum usitatissimum* L.) stem tissues. *Ann Bot* 85:477
- Gorshkova TA, Salnikov VV, Chemikosova SB, Ageeva MV, Pavlencheva NV, van Dam JEG (2003) The snap point: a transition point in *Linum usitatissimum* bast fiber development. *Ind Crops Prod* 18:213–221
- Hearle JWS (1963) The fine structure of fibers and crystalline polymers. III. Interpretation of the mechanical properties of fibers. *J Appl Polym Sci* 7:1207–1223

- Juarez C, Duran A, Valdez P, Fajardo G (2007) Performance of “*Agave lecheguilla*” natural fiber in Portland cement composites exposed to severe environment conditions. *Build Environ* 42:1151–1157
- Lehringer C, Daniel G, Schmitt U (2009) TEM/FE-SEM studies on tension wood fibres of *Acer* spp., *Fagus sylvatica* L. and *Quercus robur* L. *Wood Sci Technol* 43:691–702
- Lennholm H, Larsson T, Iversen T (1994) Determination of cellulose I[α] and I[β] in lignocellulosic materials. *Carbohydr Res* 261:119–131
- Mark RE (1967) Cell wall mechanics of tracheids. Yale University Press, New Haven
- Meredith J, Ebsworth R, Coles SR, Wood BM, Kirwan K (2012) Natural fibre composite energy absorption structures. *Compos Sci Technol* 72:211–217
- Meredith J, Coles SR, Powe R, Collings E, Cozien-Cazuc S, Weager B, Müssig J, Kirwan K (2013) On the static and dynamic properties of flax and Cordenka epoxy composites. *Compos Sci Technol* 80:31–38
- Morvan C, Andème-Onzighi C, Girault R, Himmelsbach DS, Driouch A, Akin DE (2003) Building flax fibres: more than one brick in the walls. *Plant Physiol Biochem* 41:935–944
- Mukherjee PS, Satyanarayana KG (1986a) An empirical evaluation of structure-property relationships in natural fibres and their fracture behaviour. *J Mater Sci* 21:4162–4168
- Mukherjee PS, Satyanarayana KG (1986b) Structure and properties of some vegetable fibers 2 Pineapple fiber (*Ananas comosus*). *J Mater Sci* 2:51–56
- Näslund P, Vuong R, Chanzy H, Jérior JC (1988) Diffraction contrast transmission electron microscopy on flax fiber ultrathin cross sections. *Text Res J* 58:414–417
- Nilsson T, Gustafsson PJ (2007) Influence of dislocations and plasticity on the tensile behaviour of flax and hemp fibres. *Compos A Appl Sci Manuf* 38:1722–1728
- Van den Oever MJA, Bos HL, Van Kemenade M (2000) Influence of the physical structure of flax fibres on the mechanical properties of flax fibre reinforced polypropylene composites. *Appl Compos Mater* 7:387–402
- Oksman K (2001) High quality flax fibre composites manufactured by the resin transfer moulding process. *J Reinf Plast Compos* 20:621
- Olorunnisola AO (2008) Effects of pre-treatment of rattan (*Laccosperma secundiflorum*) on the hydration of Portland cement and the development of a new compatibility index. *Cement Concr Compos* 30:37–43
- Pacheco-Torgal F, Jalali S (2011) Cementitious building materials reinforced with vegetable fibres: a review. *Constr Build Mater* 25:575–581
- Preston RD (1974) The physical biology of plant cell walls. Chapman and Hall, Londres
- Roe PJ, Ansell MP (1985) Jute-reinforced polyester composites. *J Mater Sci* 20:4015–4020
- Roland J-C, Mosiniak M, Roland D (1995) Dynamique du positionnement de la cellulose dans les parois des fibres textiles du lin (*Linum usitatissimum*). *Acta Bot Gallica* 142:463–484
- Sasaki Y, Sato S, Adachi A, Dan Y, Nishimura M (2001) Use of oolong tea extract staining of soft-tissue specimens in low-vacuum scanning electron microscope with a cooling stage. *Med Electron Microsc* 34:254–257
- Sato S, Adachi A, Satomura K (1996) The ultrastructure of spiralled collagen in liver fibrosis. *Med Electron Microsc* 29:153–158
- Sato S, Sasaki Y, Adachi A, Dai W, Liu X-L, Namimatsu S (2003) Use of oolong tea extract (OTE) for elastin staining and enhancement in ultrathin sections. *Med Electron Microsc* 36:179–182
- Sato S, Adachi A, Sasaki Y, Ghazizadeh M (2008) Oolong tea extract as a substitute for uranyl acetate in staining of ultrathin sections. *J Microsc* 229:17–20
- Sawsen C, Fouzia K, Mohamed B, Moussa G (2014) Optimizing the formulation of flax fiber-reinforced cement composites. *Constr Build Mater* 54:659–664
- Sawsen C, Fouzia K, Mohamed B, Moussa G (2015) Effect of flax fibers treatments on the rheological and the mechanical behavior of a cement composite. *Constr Build Mater* 79:229–235
- Saxena IM, Brown RM (2005) Cellulose biosynthesis: current views and evolving concepts. *Ann Bot* 96:9–21
- Sridhar MK, Basavarajappa G, Kasturi SG, Balasubramanian N (1982) Evaluation of jute as a reinforcement in composites. *Indian J Fibre Text Res* 7:87–92
- Stout HP, Jenkins JA (1955) Comparative strengths of some bast and leaf fibres. *Ann Text Belges* 4:231–251
- Thuault A, Eve S, Bazin J, Charlet K, Destaing F, Gomina M, Bréard J (2011) Morphologie, biocomposition et comportement mécanique des fibres de lin. *Matér Tech* 99(3):275–280
- Thuault A, Eve S, Blond D, Bréard J, Gomina M (2013a). Effects of the hygrothermal environment on the mechanical properties of flax fibres. *J Compos Mater* 0021998313490217
- Thuault A, Eve S, Jouannot-Chesney P, Bréard J, Gomina M (2013b) Interrelation between the variety and the mechanical properties of flax fibres. *J Biobased Mater Bioenergy* 7(5):609–618
- Thuault A, Bazin J, Eve S, Bréard J, Gomina M (2013c). Numerical study of the influence of structural and mechanical parameters on the tensile mechanical behaviour of flax fibres. *J Indu Text* 44(1):22–39
- Tröger F, Wegener G, Seemann C (1998) Miscanthus and flax as raw material for reinforced particleboards. *Ind Crops Prod* 8:113–121
- Van de Velde K, Kiekens P (2001) Thermoplastic pultrusion of natural fibre reinforced composites. *Compos Struct* 54:355–360
- Wang HH, Drummond JG, Reath SM, Hunt K, Watson PA (2001) An improved fibril angle measurement method for wood fibres. *Wood Sci Technol* 34:493–503
- Weimer PJ, Lopez-Guisa JM, French AD (1990) Effect of cellulose fine structure on kinetics of its digestion by mixed ruminal microorganisms in vitro. *Appl Environ Microbiol* 56:2421–2429
- Yamaguchi K, Suzuki K, Tanaka K (2010) Examination of electron stains as a substitute for uranyl acetate for the ultrathin sections of bacterial cells. *J Electron Microsc* 59:113
- Yan L, Chouw N (2013) Crashworthiness characteristics of flax fibre reinforced epoxy tubes for energy absorption application. *Mater Des* 51:629–640
- Yan L, Chouw N, Jayaraman K (2014a) Flax fibre and its composites—a review. *Compos B Eng* 56:296–317

- Yan L, Chouw N, Jayaraman K (2014b) Effect of triggering and polyurethane foam-filler on axial crushing of natural flax/epoxy composite tubes. *Mater Des* 56:528–541
- Yan L, Chouw N, Jayaraman K (2014c) Lateral crushing of empty and polyurethane-foam filled natural flax fabric reinforced epoxy composite tubes. *Compos B Eng* 63:15–26

- Yan L, Chouw N, Jayaraman K (2015) Effect of UV and water spraying on the mechanical properties of flax fabric reinforced polymer composites used for civil engineering applications. *Mater Des* 71:17–25